



ALMA MATER STUDIORUM  
UNIVERSITÀ DI BOLOGNA

ARCHIVIO ISTITUZIONALE  
DELLA RICERCA

## Alma Mater Studiorum Università di Bologna Archivio istituzionale della ricerca

Ca<sup>2+</sup> as cofactor of the mitochondrial H<sup>+</sup>-translocating F<sub>1</sub>F<sub>0</sub>-ATP(hydrol)ase

This is the final peer-reviewed author's accepted manuscript (postprint) of the following publication:

*Published Version:*

Nesci S., Pagliarani A. (2021). Ca<sup>2+</sup> as cofactor of the mitochondrial H<sup>+</sup>-translocating F<sub>1</sub>F<sub>0</sub>-ATP(hydrol)ase. *PROTEINS*, 869(5), 477-482 [10.1002/prot.26040].

*Availability:*

This version is available at: <https://hdl.handle.net/11585/817907> since: 2021-04-03

*Published:*

DOI: <http://doi.org/10.1002/prot.26040>

*Terms of use:*

Some rights reserved. The terms and conditions for the reuse of this version of the manuscript are specified in the publishing policy. For all terms of use and more information see the publisher's website.

This item was downloaded from IRIS Università di Bologna (<https://cris.unibo.it/>).  
When citing, please refer to the published version.

(Article begins on next page)

This is the final peer-reviewed accepted manuscript of:

**Ca<sup>2+</sup> as cofactor of the mitochondrial H<sup>+</sup>-translocating F<sub>1</sub>F<sub>0</sub>-ATP(hydrol)ase.**

**Nesci S, Pagliarani A. Proteins, 89: 477–482.**

The final published version is available online at:  
<http://dx.doi.org/10.1002/prot.26040>

Rights / License:

The terms and conditions for the reuse of this version of the manuscript are specified in the publishing policy. For all terms of use and more information see the publisher's website.

*This item was downloaded from IRIS Università di Bologna (<https://cris.unibo.it/>)*

***When citing, please refer to the published version.***

1  
2  
3  $\text{Ca}^{2+}$  as cofactor of the mitochondrial  $\text{H}^+$ -translocating  $\text{F}_1\text{F}_\text{O}$ -ATP(hydrol)ase  
4  
5  
6  
7

8  
9 *Salvatore Nesci, Alessandra Pagliarani*

10 Department of Veterinary Medical Sciences, University of Bologna, Ozzano Emilia Via Tolara di  
11  
12 Sopra 50, 40064 Bologna, Italy.

13  
14  
15 Corresponding author: [salvatore.nesci@unibo.it](mailto:salvatore.nesci@unibo.it)  
16  
17  
18  
19  
20  
21  
22

23 Running title:  $\text{H}^+$ -translocation driven by ATP hydrolysis by the  $\text{Ca}^{2+}$ -activated  $\text{F}_1\text{F}_\text{O}$ -ATPase  
24  
25  
26  
27

28 **Abstract**  
29

30  
31 The mitochondrial  $\text{F}_1\text{F}_\text{O}$ -ATPase in the presence of the natural cofactor  $\text{Mg}^{2+}$  acts as the enzyme of  
32 life by synthesizing ATP, but it can also hydrolyze ATP to pump  $\text{H}^+$ . Interestingly,  $\text{Mg}^{2+}$  can be  
33 replaced by  $\text{Ca}^{2+}$ , but only to sustain ATP hydrolysis and not ATP synthesis. When  $\text{Ca}^{2+}$  inserts in  
34  $\text{F}_1$ , the torque generation built by the chemomechanical coupling between  $\text{F}_1$  and the rotating central  
35 stalk was reported as unable to drive the transmembrane  $\text{H}^+$  flux within  $\text{F}_\text{O}$ . However, the failed  $\text{H}^+$   
36 translocation is not consistent with the oligomycin-sensitivity of the  $\text{Ca}^{2+}$ -dependent  $\text{F}_1\text{F}_\text{O}$ -  
37 ATP(hydrol)ase. New enzyme roles in mitochondrial energy transduction are suggested by recent  
38 advances. Accordingly, the structural  $\text{F}_1\text{F}_\text{O}$ -ATPase distortion driven by ATP hydrolysis sustained by  
39  $\text{Ca}^{2+}$  is consistent with the permeability transition pore signal propagation pathway. The  $\text{Ca}^{2+}$ -  
40 activated  $\text{F}_1\text{F}_\text{O}$ -ATPase, by forming the pore, may contribute to dissipate the transmembrane  $\text{H}^+$   
41 gradient created by the same enzyme complex.  
42  
43  
44  
45  
46  
47  
48  
49  
50  
51  
52  
53

54  
55  
56  
57  
58 **Keywords:**  $\text{Ca}^{2+}$  cofactor;  $\text{F}_1\text{F}_\text{O}$ -ATPase; mitochondria;  $\text{H}^+$  pump; oligomycin; permeability transition  
59 pore; bioenergetics.  
60

## 1. Introduction

The mitochondrial  $F_1F_0$ -ATPase is a multisubunit complex arranged in dimers or oligomers and placed at the edge of the *cristae* of the inner mitochondrial membrane (IMM) <sup>1</sup>. The monomer is formed by two domains, named  $F_1$  and  $F_0$  functionally and structurally linked to a stator (lateral stalk) and a rotor (central stalk). The  $F_1$  portion, namely the hydrophilic domain that protrudes in the mitochondrial matrix, has a conspicuous lollipop shape formed by  $\alpha_3$ ,  $\beta_3$ ,  $\gamma$ ,  $\delta$ , and  $\epsilon$  subunits. An alternated arrangement of  $\alpha$  and  $\beta$  subunits forms a globular hexamer around the  $\gamma$  subunit (Fig. 1A). The structure functions as a reversible rotary molecular motor which can build or hydrolyze ATP depending on the rotation direction, which in turn is driven by the transmembrane proton-motive force ( $\Delta p$ ). *In vitro* the  $\gamma$  subunit of  $F_1$ -ATPase was shown to rotate within the surrounding  $\alpha_3\beta_3$  subunits, synthesizing or hydrolysing ATP in three separate catalytic sites on the  $\alpha/\beta$  subunit interface. The catalytic sites are alternated with the non-catalytic sites, which can only bind adenine nucleotides <sup>2</sup>. During the kinetic reactions, the three non-equivalent conformation  $\beta_E$  (empty),  $\beta_{DP}$  (which hosts ADP) and  $\beta_{TP}$  (contains ATP or ADP) of the catalytic sites, with increasing affinity for ATP, change their conformation and binding properties every  $120^\circ$  with the rotation of the rotor <sup>3</sup>. In addition, the  $F_1F_0$ -ATPase catalytic and non-catalytic sites in their different conformations can also bind metal divalent cations <sup>1</sup>. In mammals, the membrane-embedded domain is composed by the  $a$  subunit, the transmembrane  $\alpha$ -helices of  $b$  subunit, the  $c_n$  subunits ( $n=$  eight in mammals) which arranged as a cylindric palisade form the  $c$ -ring, A6L subunit, and the supernumerary subunits  $e$ ,  $f$ ,  $g$ , DAPIT (Diabetes-Associated Protein in Insulin-sensitive Tissue), 6.8 KDa proteolipid (PL) (Fig. 1A) <sup>4</sup>. The  $H^+$  translocation sector arises from  $a/c$ -ring interactions by forming two asymmetric half-channels with unexpected horizontal membrane-intrinsic  $\alpha$ -helices in the  $a$  subunit. These two half-channels are mutually offset, while the  $H^+$  binding sites are located on the C-terminal  $\alpha$ -helix of each  $c$  subunit <sup>5</sup>. In the mammalian  $F_1F_0$ -ATPase the  $a$  and A6L membrane subunits are encoded by the mitochondrial DNA. The central stalk within the  $F_1$  domain contains the  $\gamma$  subunit, which joined to the  $\delta$  and  $\epsilon$  subunits, forms a sort of foot which interacts with the loop region of  $c$ -ring. The lateral or peripheral stalk joins the two  $F_0$  and  $F_1$  enzyme domains (Fig. 1A). The  $b$  subunit spans the complete length of the lateral stalk and interacts with OSCP, F6 and  $d$  subunits which belong to the soluble

1  
2  
3 enzyme section. All these subunits connect the soluble stator subunits with  $\alpha_{TP}$  subunit of  $F_1$  domain.  
4  
5 In addition, the top of  $\alpha_{TP}$ ,  $\alpha_{DP}$ ,  $\alpha_E$  and the  $\beta_{DP}$  and  $\beta_E$  are only linked with OSCP. Some subunits of  
6  
7 the lateral stalk, namely the membrane embedded portion of  $b$ ,  $f$  and A6L subunits <sup>6</sup> and the  
8  
9 supernumerary subunits, are transmembrane subunits <sup>4</sup>. The lateral stalk shows a spectacular  
10  
11 flexibility that plays the role of resisting the torque generation of the rotor by coupling  $F_1$  catalysis to  
12  
13  $H^+$  translocation <sup>7,8</sup>.  
14

15  
16 The  $H^+$ -translocating  $F_1F_0$ -ATPase sustains either ATP synthesis or hydrolysis <sup>9</sup>. In the “forward”  
17  
18 mode the Mitchell’s proton motive force  $\Delta p$  created by mitochondrial respiration drives ATP formation  
19  
20 from ADP and  $P_i$ . In the so-called “reverse” mode, the phosphorylation potential generated by ATP  
21  
22 breakdown is exploited by the enzyme complex to pump  $H^+$  and energize the IMM when the  $\Delta p$   
23  
24 drops <sup>10</sup>. Both ATP synthase and hydrolase activities are opposite  $F_1F_0$ -ATPase functions that  
25  
26 depend on the bioenergetic state of mitochondria. The bi-functional ATP synthesis/hydrolysis mode  
27  
28 coupled to  $H^+$  translocation of  $F_1F_0$ -ATPase is a mechanism unique in biology sustained by the  
29  
30 natural cofactor  $Mg^{2+}$ . The  $F_1F_0$ -ATPase can replace  $Mg^{2+}$  by  $Ca^{2+}$  losing the ATP synthesis function,  
31  
32 but preserving the  $F_1F_0$ -ATP(hydrol)ase activity <sup>11</sup>. High  $Ca^{2+}$  concentrations in mitochondria activate  
33  
34 of  $F_1F_0$ -ATPase by direct  $Ca^{2+}$  binding to the  $\alpha_3\beta_3$  globular hexamer that dissociates ATP hydrolysis  
35  
36 from  $H^+$  pumping. In this case  $F_1$  was reported to become uncoupled from  $F_0$  domain <sup>12</sup>. However,  
37  
38 this assumption becomes questionable on considering the recent cryo-EM enzyme structure and  
39  
40 structure activity relationship data on the effect of small molecules <sup>13</sup> and specific  $F_1$  and  $F_0$  domain  
41  
42 inhibitors <sup>11,14</sup>. So, in search for a different interpretation of the findings up to now obtained,  
43  
44 experimental and literature data <sup>15</sup> were combined to draw a pattern of the mechanism involved.  
45  
46  
47  
48  
49  
50

## 51 2. Materials and Methods

### 52 2.1. Preparation of the mitochondrial fractions and $F_1F_0$ -ATPase activity assays

53  
54 Swine hearts (*Sus scrofa domesticus*) were collected at a local abattoir and transported to the lab.  
55  
56 From homogenized heart tissue and then subjected to differential centrifugation <sup>11</sup> the mitochondrial  
57  
58 preparations, obtained in a divalent cation-free medium, were characterized as described in <sup>14</sup>. To  
59  
60

1  
2  
3 evaluate the mitochondrial  $F_1F_0$ -ATPase activities, the mitochondrial preparations obtained as  
4 described by Nesci et al. <sup>11</sup>, were added to the reaction system that contained 3 mM ATP and 2 mM  
5  $Ca^{2+}$  or  $Mg^{2+}$  in 75 mM ethanolamine-HCl buffer, pH 8.8. The enzyme activity was  
6 spectrophotometrically detected and evaluated after subtraction of the non-specific ATP hydrolysis  
7 in the blank<sup>16</sup>. The sensitivity of the  $F_1F_0$ -ATPase activity, either sustained by  $Mg^{2+}$  or by  $Ca^{2+}$ , to the  
8 specific  $F_1F_0$ -ATPase inhibitor oligomycin witnessed the functional and structural coupling between  
9 the two sectors  $F_1$  and  $F_0$  <sup>14</sup>.  
10  
11  
12  
13  
14  
15  
16  
17  
18  
19  
20

## 21 2.2. Protein model

22  
23 The structural details of the protein arrangement in the  $F_1F_0$ -ATPase subunits were obtained by the  
24 Chem3D program of ChemOffice Professional 19.1.1 software <sup>17</sup> using the deposited structures in  
25 PDB.  
26  
27  
28  
29  
30  
31  
32

## 33 2.3. Calculations and statistics

34  
35 In each set of experiments, the data represent the mean  $\pm$  SD of the number of analyses carried out  
36 on at least three distinct mitochondrial preparations. The coupling index was calculated as the ratio  
37 between the total  $F_1F_0$ -ATPase activity and the oligomycin-sensitive  $F_1F_0$ -ATPase activity, being the  
38 latter obtained from the difference between the total  $F_1F_0$ -ATPase activity and the enzyme activity  
39 detected in the presence of 3mg/mL oligomycin, a dose which ensured maximal inhibition of the  
40  $F_1F_0$ -ATPase <sup>18</sup>. The differences between the enzyme activity data in differently treated mitochondria  
41 were evaluated by one way ANOVA followed by Student-Newman-Keuls' test when  $F$  values  
42 indicated significance ( $P \leq 0.05$ ). The significance of the difference between the mean coupling index  
43 of the  $Mg^{2+}$ -dependent  $F_1F_0$ -ATPase and the  $Ca^{2+}$ -dependent  $F_1F_0$ -ATPase was evaluated by  
44 Student's  $t$  test ( $P \leq 0.05$ ). Percentage data were *arcsin*-transformed before statistical analyses to  
45 ensure normality.  
46  
47  
48  
49  
50  
51  
52  
53  
54  
55  
56  
57  
58  
59  
60

### 3. Results and Discussion

The catalytic and non-catalytic subunits of the  $F_1F_0$ -ATPase show specific amino acid residues and secondary structure motifs required for the molecular interaction with adenine nucleotides and divalent cations. An eight amino acids sequence, *GXXXXGKT*, conserved in all ATPases<sup>19</sup> is the basic structural feature of the P-loop, known as a phosphate binding loop, on  $\alpha$  and  $\beta$  subunits (Fig. 1B). The motif interacts with  $Mg^{2+}$  and phosphate (Pi) groups of ATP by coordinating  $\beta$ -Pi and  $\gamma$ -Pi to exchange the terminal  $\gamma$ -Pi when the ATP is synthesized or hydrolysed. The positions and specific amino acid composition in the pig sequence are  $_{158}GGAGVGKT_{165}$  and  $_{169}GDRGTGKT_{176}$  in the  $\beta$  and  $\alpha$  subunits, respectively.  $T_{165}$  is the only residue that plays a key role in coordinating  $Mg^{2+}$  in the  $\beta$  subunits of enzyme during ATP hydrolysis, while  $T_{176}$  of  $\alpha$  subunits could bind the cofactor. Similarly to  $Mg^{2+}$ ,  $Ca^{2+}$  can also bind to all the catalytic sites and probably also to the non-catalytic sites<sup>4</sup>. The relative affinities for divalent cations and ATP in the reverse reaction of ATP hydrolysis are modulated by mutagenesis of these specific residues of  $\beta$  subunits<sup>20</sup>. However,  $Ca^{2+}$ , which has higher steric hindrance than  $Mg^{2+}$ , can change the coordination geometry of the  $Mg^{2+}$ -binding site from the octahedral bipyramide which binds six ligands up to allow eight ligands when  $Ca^{2+}$  is inserted in replacement of  $Mg^{2+}$ <sup>21</sup>. Therefore, the rigid octahedral complex changes to a less rigid geometry with irregular bond distances and angles and variable coordination number. This flexible arrangement may explain the non-competitive  $Ca^{2+}$  inhibition of the  $Mg^{2+}$ -activated  $F_1F_0$ -ATPase<sup>14</sup>. The  $Ca^{2+}$ -dependent  $F_1F_0$ -ATP(hydrol)ase is capable of sustaining torque generation of the rotor. The rotational motion was found to be similar to that induced by  $Mg^{2+}$  in the  $F_1$ -ATPase<sup>22</sup>.  $Ca^{2+}$  binding could have the functional consequence to prevent the building of the transmembrane  $H^+$  gradient, as shown by ACMA fluorescence quenching<sup>23</sup>. However, these results cannot exclude that the rotation driven by ATP hydrolysis stimulated by  $Ca^{2+}$ <sup>22</sup> is coupled to  $H^+$  translocation. The  $Mg^{2+}$ -activated  $F_1F_0$ -ATPase can display  $H^+$  flow across  $F_0$  in the absence of adenine nucleotides bound to  $F_1$ . This uncoupled proton leakage, known as "proton slip", is associated with a free-wheeling of the central stalk under non-physiological conditions<sup>10</sup>. In addition, the proton slip is abolished by  $F_0$  inhibitors (e.g. oligomycin), but it is insensitive to  $F_1$  inhibitors. Conversely, the  $Ca^{2+}$ -dependent  $F_1F_0$ -ATP(hydrol)ase activity was shown to inhibited by various  $F_1$  inhibitors<sup>14</sup> and insensitive to other Ca-

1  
2  
3 ATPase inhibitors <sup>24</sup>. Since the  $F_1F_0$ -ATPase in the presence of  $Ca^{2+}$  shows a four orders of  
4 magnitude lower enzyme activity than the  $Mg^{2+}$ -activated  $F_1F_0$ -ATPase (Fig. 2A), ATP hydrolysis  
5 sustained by  $Ca^{2+}$  may be unable to support a significant  $H^+$  pumping to energize the membrane.  
6  
7 Moreover, the  $Ca^{2+}$ -activated  $F_1F_0$ -ATPase is now generally recognized to play an important role in  
8 the permeability transition pore (PTP) formation and opening <sup>25-29</sup>, which can dissipate the  $\Delta p$  <sup>11</sup>. The  
9 loss of  $F_1F_0$ -ATPase structural-functional integrity emerges as the most likely event involved in the  
10 decreased oligomycin sensitivity when the  $F_1$  catalysis is not coupled to  $H^+$  transport by  $F_0$  <sup>30</sup>.  
11 However, the  $Ca^{2+}$ -dependent  $F_1F_0$ -ATP(hydrol)ase is inhibited by oligomycin <sup>24</sup>. A similar behaviour  
12 was described in pea stem mitochondria, where, since the Ca-ATPase activity was fully sensitive to  
13 oligomycin, ATP hydrolysis could be coupled to  $H^+$  translocation <sup>31</sup>. In swine heart mitochondria  
14 oligomycin displays a higher inhibition efficiency on the  $Ca^{2+}$ -activated  $F_1F_0$ -ATPase than on the  
15  $Mg^{2+}$ -activated  $F_1F_0$ -ATPase, as shown by the lower  $IC_{50}$  value (Fig. 2B). The coupling index (the  
16 ratio between the total  $F_1F_0$ -ATPase activity and the oligomycin-sensitive  $F_1F_0$ -ATPase activity) is  
17 statistically similar, namely  $94.7 \pm 1.8\%$  and  $91.6 \pm 3.7\%$  in presence of  $Mg^{2+}$  and  $Ca^{2+}$ , respectively.  
18 Therefore oligomycin blocks  $H^+$  translocation coupled to ATP hydrolysis irrespective of the divalent  
19 cation (Fig. 2C). Consistently, these data suggest that mechanochemical coupling of  $Ca^{2+}$ -  
20 dependent  $F_1$ -ATP(hydrol)ase works as a rotary chemical motor to drive  $H^+$  translocation in the  $F_0$   
21 domain <sup>11,16</sup>. The fact that the  $H^+$ -pumping activity driven by  $Ca^{2+}$  may not energize IMM is not  
22 surprising, being supported by the new "bent-pull" model of the c-ring gated channel <sup>32</sup> and by the  
23 cryo-EM maps of the enzyme exposed to  $Ca^{2+}$  <sup>4</sup>. The lack of apparent  $H^+$  translocation with  $Ca^{2+}$ -  
24 dependent  $F_1F_0$ -ATP(hydrol)ase may be rather due to  $H^+$  backflow through the open PTP <sup>33</sup>. Indeed,  
25 different  $Ca^{2+}$   $F_1F_0$ -ATPase states during ATP hydrolysis were not identified in the  $Mg^{2+}$ -activated  
26  $F_1F_0$ -ATPase. Moreover recent data show that the PTP opens when the  $Ca^{2+}$ -enzyme in  
27 disassembled conformation has the peripheral stalk twisted and the  $F_1$  detached from  $F_0$  <sup>4</sup> (Fig. 3).  
28 In all likelihood, oligomycin inhibits ATP hydrolysis sustained by  $Ca^{2+}$  in the first conformational  
29 stages of the  $Ca^{2+}$ -dependent  $F_1F_0$ -ATP(hydrol)ase when  $F_1$  is still coupled to  $F_0$ . Indeed,  
30 oligomycin, venturicidin, and DCCD, which block  $H^+$  translocation by binding to the c-ring, can reduce  
31 the calcein quenching rate <sup>34</sup>, while small-molecules obtained from the oligomycin structure target

1  
2  
3 the *c* subunits and inhibit the PTP<sup>35</sup>. Previous experiments in our lab showed that DCCD, which  
4 specifically blocks H<sup>+</sup> translocation by covalently binding to the *c* subunit carboxylic groups which  
5 constitute H<sup>+</sup> binding sites and inhibits ATP hydrolysis, more promptly reacts and binds to the Ca<sup>2+</sup>-  
6 activated F<sub>1</sub>F<sub>0</sub>-ATPase than the Mg<sup>2+</sup>-activated F<sub>1</sub>F<sub>0</sub>-ATPase<sup>11</sup>. Moreover, in inside-out  
7 submitochondrial particles the oligomycin sensitive ATP hydrolysis was shown to be similarly  
8 affected by Δ*p* when the enzyme activity is sustained by Ca<sup>2+</sup> or by Mg<sup>2+</sup><sup>11</sup>. Therefore, most likely,  
9 when the activating cation is Ca<sup>2+</sup>, H<sup>+</sup> translocation may be masked by the high ionic conductance  
10 of the open PTP.  
11  
12  
13  
14  
15  
16  
17  
18  
19

20 To sum up, the H<sup>+</sup>-translocating Ca<sup>2+</sup>-dependent F<sub>1</sub>F<sub>0</sub>-ATP(hydrol)ase is a (mono)functional mode  
21 of the mitochondrial F-type ATPase complex. The F<sub>1</sub> domain which hydrolyzes ATP in the presence  
22 of Ca<sup>2+</sup> drives the mechanical-power transmission which results in F<sub>0</sub> conductance to H<sup>+</sup>.  
23 Consistently, the poor H<sup>+</sup>-pumping activity of the Ca<sup>2+</sup>-dependent F<sub>1</sub>F<sub>0</sub>-ATP(hydrol)ase fails to  
24 energize the IMM, mainly because the same enzyme activity is a key PTP constituent, and most  
25 likely the PTP opening prevents and masks Δ*p* formation<sup>33,36</sup>.  
26  
27  
28  
29  
30  
31  
32  
33  
34  
35  
36

#### 37 4. Conclusion

38  
39 Since long-time Ca<sup>2+</sup> has been involved in the F<sub>1</sub>F<sub>0</sub>-ATPase modulation in heart mitochondria<sup>37</sup>.  
40 Most knowledge comes from *in vitro* experiments, mainly due to difficulties in the detection of  
41 individual action mechanisms *in vivo*<sup>38</sup>. The structural data which cast light on the Ca<sup>2+</sup>-driven  
42 conformational changes of the F<sub>1</sub>F<sub>0</sub>-ATPase shoulder the idea that, among the multiple Ca<sup>2+</sup> actions  
43 in mitochondria, the Ca<sup>2+</sup> intervention in the PTP is one of the most relevant mitochondrial roles of  
44 this multitasking cation in physiology and pathology.  
45  
46  
47  
48  
49  
50  
51  
52  
53  
54  
55  
56  
57

#### 58 Conflicts of interest

59 None.  
60

## Acknowledgments

This work was supported by the CARISBO Foundation Grants n° 2019.0534, Bologna, Italy to SN.

## References

- 1 Hahn A, Parey K, Bublitz M, Mills DJ, Zickermann V, Vonck J *et al.* Structure of a Complete ATP Synthase Dimer Reveals the Molecular Basis of Inner Mitochondrial Membrane Morphology. *Mol Cell* 2016; **63**: 445–456.
- 2 Boyer PD. The ATP synthase--a splendid molecular machine. *Annu Rev Biochem* 1997; **66**: 717–749.
- 3 Yoshida M, Muneyuki E, Hisabori T. ATP synthase--a marvellous rotary engine of the cell. *Nat Rev Mol Cell Biol* 2001; **2**: 669–677.
- 4 Pinke G, Zhou L, Sazanov LA. Cryo-EM structure of the entire mammalian F-type ATP synthase. *Nat Struct Mol Biol* 2020. doi:10.1038/s41594-020-0503-8.
- 5 Nesci S, Pagliarani A, Algieri C, Trombetti F. Mitochondrial F-type ATP synthase: multiple enzyme functions revealed by the membrane-embedded FO structure. *Crit Rev Biochem Mol Biol* 2020; : 1–13.
- 6 Gu J, Zhang L, Zong S, Guo R, Liu T, Yi J *et al.* Cryo-EM structure of the mammalian ATP synthase tetramer bound with inhibitory protein IF1. *Science* 2019; **364**: 1068–1075.
- 7 Hahn A, Vonck J, Mills DJ, Meier T, Kühlbrandt W. Structure, mechanism, and regulation of the chloroplast ATP synthase. *Science* 2018; **360**: eaat4318.
- 8 Junge W, Sielaff H, Engelbrecht S. Torque generation and elastic power transmission in the rotary F(O)F(1)-ATPase. *Nature* 2009; **459**: 364–370.
- 9 Junge W, Lill H, Engelbrecht S. ATP synthase: An electrochemical transducer with rotatory mechanics. *Trends in Biochemical Sciences* 1997; **22**: 420–423.
- 10 Feniouk BA, Mulkidjanian AY, Junge W. Proton slip in the ATP synthase of *Rhodobacter capsulatus*: induction, proton conduction, and nucleotide dependence. *Biochim Biophys Acta* 2005; **1706**: 184–194.
- 11 Nesci S, Trombetti F, Ventrella V, Pirini M, Pagliarani A. Kinetic properties of the mitochondrial F1FO-ATPase activity elicited by Ca(2+) in replacement of Mg(2+). *Biochimie* 2017; **140**: 73–81.
- 12 Hubbard MJ, McHugh NJ. Mitochondrial ATP synthase F1-beta-subunit is a calcium-binding protein. *FEBS Lett* 1996; **391**: 323–329.

1  
2  
3  
4  
5  
6  
7  
8  
9  
10  
11  
12  
13  
14  
15  
16  
17  
18  
19  
20  
21  
22  
23  
24  
25  
26  
27  
28  
29  
30  
31  
32  
33  
34  
35  
36  
37  
38  
39  
40  
41  
42  
43  
44  
45  
46  
47  
48  
49  
50  
51  
52  
53  
54  
55  
56  
57  
58  
59  
60

- 13 Algieri V, Algieri C, Maiuolo L, De Nino A, Pagliarani A, Tallarida MA *et al.* 1,5-Disubstituted-1,2,3-triazoles as inhibitors of the mitochondrial Ca<sup>2+</sup>-activated F<sub>1</sub>FO-ATP(hydrol)ase and the permeability transition pore. *Ann N Y Acad Sci* 2020. doi:10.1111/nyas.14474.
- 14 Algieri C, Trombetti F, Pagliarani A, Ventrella V, Bernardini C, Fabbri M *et al.* Mitochondrial Ca<sup>2+</sup>-activated F<sub>1</sub>FO-ATPase hydrolyzes ATP and promotes the permeability transition pore. *Ann N Y Acad Sci* 2019; **1457**: 142–157.
- 15 Nesci S, Pagliarani A. Incoming news on the F-type ATPase structure and functions in mammalian mitochondria. *Biochimica et Biophysica Acta - Advances* 2021. doi:10.1016/j.bbadv.2020.100001.
- 16 Algieri C, Trombetti F, Pagliarani A, Ventrella V, Nesci S. Phenylglyoxal inhibition of the mitochondrial F<sub>1</sub>FO-ATPase activated by Mg<sup>2+</sup> or by Ca<sup>2+</sup> provides clues on the mitochondrial permeability transition pore. *Arch Biochem Biophys* 2020; **681**: 108258.
- 17 Trombetti F, Pagliarani A, Ventrella V, Algieri C, Nesci S. Crucial aminoacids in the FO sector of the F<sub>1</sub>FO-ATP synthase address H<sup>+</sup> across the inner mitochondrial membrane: molecular implications in mitochondrial dysfunctions. *Amino Acids* 2019; **51**: 579–587.
- 18 Nesci S, Ventrella V, Trombetti F, Pirini M, Pagliarani A. Thiol oxidation is crucial in the desensitization of the mitochondrial F<sub>1</sub>FO-ATPase to oligomycin and other macrolide antibiotics. *Biochim Biophys Acta* 2014; **1840**: 1882–1891.
- 19 Ramakrishnan C, Dani VS, Ramasarma T. A conformational analysis of Walker motif A [GXXXXGKT (S)] in nucleotide-binding and other proteins. *Protein Eng* 2002; **15**: 783–798.
- 20 Du Z, Tucker WC, Richter ML, Gromet-Elhanan Z. Assembled F<sub>1</sub>-(alpha beta) and Hybrid F<sub>1</sub>-alpha 3beta 3gamma-ATPases from *Rhodospirillum rubrum* alpha, wild type or mutant beta, and chloroplast gamma subunits. Demonstration of Mg<sup>2+</sup>-versus Ca<sup>2+</sup>-induced differences in catalytic site structure and function. *J Biol Chem* 2001; **276**: 11517–11523.
- 21 Casadio R, Melandri BA. CaATP inhibition of the MgATP-dependent proton pump (H<sup>+</sup>-ATPase) in bacterial photosynthetic membranes with a mechanism of alternative substrate inhibition. *JBIC* 1996; **1**: 284–291.
- 22 Tucker WC, Schwarz A, Levine T, Du Z, Gromet-Elhanan Z, Richter ML *et al.* Observation of calcium-dependent unidirectional rotational motion in recombinant photosynthetic F<sub>1</sub>-ATPase molecules. *J Biol Chem* 2004; **279**: 47415–47418.
- 23 Papageorgiou S, Melandri AB, Solaini G. Relevance of divalent cations to ATP-driven proton pumping in beef heart mitochondrial F<sub>0</sub>F<sub>1</sub>-ATPase. *J Bioenerg Biomembr* 1998; **30**: 533–541.
- 24 Nesci S, Ventrella V, Trombetti F, Pirini M, Pagliarani A. Preferential nitrite inhibition of the mitochondrial F<sub>1</sub>FO-ATPase activities when activated by Ca(2+) in replacement of the natural cofactor Mg(2+). *Biochim Biophys Acta* 2016; **1860**: 345–353.
- 25 Alavian KN, Beutner G, Lazrove E, Sacchetti S, Park H-A, Licznerski P *et al.* An uncoupling channel within the c-subunit ring of the F<sub>1</sub>FO ATP synthase is the mitochondrial permeability transition pore. *Proc Natl Acad Sci USA* 2014; **111**: 10580–10585.
- 26 Bonora M, Bononi A, De Marchi E, Giorgi C, Lebiedzinska M, Marchi S *et al.* Role of the c subunit of the FO ATP synthase in mitochondrial permeability transition. *Cell Cycle* 2013; **12**: 674–683.

- 1  
2  
3 27 Giorgio V, von Stockum S, Antoniel M, Fabbro A, Fogolari F, Forte M *et al.* Dimers of  
4 mitochondrial ATP synthase form the permeability transition pore. *Proc Natl Acad Sci USA*  
5 2013; **110**: 5887–5892.  
6  
7 28 Mnatsakanyan N, Llaguno MC, Yang Y, Yan Y, Weber J, Sigworth FJ *et al.* A mitochondrial  
8 megachannel resides in monomeric F1FO ATP synthase. *Nat Commun* 2019; **10**: 5823.  
9  
10 29 Urbani A, Giorgio V, Carrer A, Franchin C, Arrigoni G, Jiko C *et al.* Purified F-ATP synthase  
11 forms a Ca<sup>2+</sup>-dependent high-conductance channel matching the mitochondrial permeability  
12 transition pore. *Nat Commun* 2019; **10**: 4341.  
13  
14 30 Devenish RJ, Prescott M, Boyle GM, Nagley P. The Oligomycin Axis of Mitochondrial ATP  
15 Synthase: OSCP and the Proton Channel. *J Bioenerg Biomembr* 2000; **32**: 507–515.  
16  
17 31 De Col V, Petrusa E, Casolo V, Braidot E, Lippe G, Filippi A *et al.* Properties of the  
18 Permeability Transition of Pea Stem Mitochondria. *Front Physiol* 2018; **9**: 1626.  
19  
20 32 Mnatsakanyan N, Jonas EA. ATP synthase c-subunit ring as the channel of mitochondrial  
21 permeability transition: Regulator of metabolism in development and degeneration. *J Mol Cell*  
22 *Cardiol* 2020; **144**: 109–118.  
23  
24 33 Bernardi P, Rasola A, Forte M, Lippe G. The Mitochondrial Permeability Transition Pore:  
25 Channel Formation by F-ATP Synthase, Integration in Signal Transduction, and Role in  
26 Pathophysiology. *Physiol Rev* 2015; **95**: 1111–1155.  
27  
28 34 Bonora M, Morganti C, Morciano G, Pedriali G, Lebedzinska-Arciszewska M, Aquila G *et al.*  
29 Mitochondrial permeability transition involves dissociation of F1FO ATP synthase dimers and  
30 C-ring conformation. *EMBO Rep* 2017; **18**: 1077–1089.  
31  
32 35 Morciano G, Preti D, Pedriali G, Aquila G, Missiroli S, Fantinati A *et al.* Discovery of Novel  
33 1,3,8-Triazaspiro[4.5]decane Derivatives That Target the c Subunit of F1/FO-Adenosine  
34 Triphosphate (ATP) Synthase for the Treatment of Reperfusion Damage in Myocardial  
35 Infarction. *J Med Chem* 2018; **61**: 7131–7143.  
36  
37 36 Nesci S. The mitochondrial permeability transition pore in cell death: A promising drug binding  
38 bioarchitecture. *Medicinal Research Reviews* 2020; **40**: 811–817.  
39  
40 37 Balaban RS. Cardiac energy metabolism homeostasis: role of cytosolic calcium. *J Mol Cell*  
41 *Cardiol* 2002; **34**: 1259–1271.  
42  
43 38 Glancy B, Balaban RS. Role of mitochondrial Ca<sup>2+</sup> in the regulation of cellular energetics.  
44 *Biochemistry* 2012; **51**: 2959–2973.  
45  
46  
47  
48  
49  
50  
51  
52  
53  
54  
55  
56  
57  
58  
59  
60

1  
2  
3 Figure 1. Representative structure of  $F_1F_0$ -ATPase monomers in mammalian mitochondria (A). The  
4 enzyme subunits are drawn as ribbon representations obtained from modified PDB ID codes: 6TT7.  
5  $\Delta p$ , Mitchell's proton motive force, IMM, inner mitochondrial membrane. The letter colors are the  
6 same as those of the subunit to which belong. B) Catalytic binding site of  $F_1F_0$ -ATPase. The ATP  
7 substrate and  $Mg^{2+}$  cofactor (in ball and stick representation) are located in the  $\beta$  and  $\alpha$  subunits,  
8 drawn as ribbon model (modified PDB ID code: 6J5J) in  $\beta_{TP}$  and  $\alpha_{TP}$  conformation, respectively,  
9 which show the position of key amino acid residues that bind  $Mg^{2+}$ . The P-loop is in light blue in both  
10 subunits. The binding sites are viewed from the  $\gamma$  subunit (upper panel) and between the observer  
11 and the  $\gamma$  subunit (lower panel).

22  
23  
24  
25 Figure 2. Effect of divalent cations on ATP hydrolysis by the mitochondrial  $F_1F_0$ -ATPase. A)  $F_1F_0$ -  
26 ATPase activities in the presence of  $Ca^{2+}$  or  $Mg^{2+}$  are shown as bar chart. B) Dose-response curve  
27 of oligomycin on the  $F_1F_0$ -ATPase activated by  $Ca^{2+}$  or  $Mg^{2+}$  expressed as percentage of the enzyme  
28 activity in the absence of oligomycin. C) The oligomycin-sensitive ATPase activity (■) and the  
29 oligomycin-insensitive ATPase activity in presence of 3  $\mu g/ml$  of oligomycin (■) are expressed as  
30 percentages of the total mitochondrial ATPase activity sustained by  $Ca^{2+}$  or  $Mg^{2+}$ , respectively. Data  
31 expressed as column chart represent the mean  $\pm$  SD (vertical bars) from three experiments carried  
32 out on different mitochondrial preparations. \* indicates significantly different values ( $P \leq 0.05$ ).

33  
34  
35  
36  
37  
38  
39  
40  
41  
42  
43  
44  
45 Figure 3.  $F_1F_0$ -ATPase activity raised by  $Mg^{2+}$  or  $Ca^{2+}$  as cofactors. ATP hydrolysis sustained by  
46  $Mg^{2+}$  (i) or  $Ca^{2+}$  (ii) is coupled to  $H^+$  translocation. The different size of the two cofactors changes the  
47  $F_1F_0$ -ATPase conformation. Indeed, the transition of the  $Ca^{2+}$ -dependent  $F_1F_0$ -ATP(hydrol)ase from  
48 the assembled (ii) to the disassembled state (iii) could induce the loss of  $H^+$ -translocation.  
49 Consequently, the PTP opens when a retracted e subunit pulls the lyso-phosphatidylserine plug out  
50 of the c-ring at the inner mitochondrial membrane side, while the  $F_1F_0$  destabilization pulls out  
51 phosphatidylserine at the matrix side.

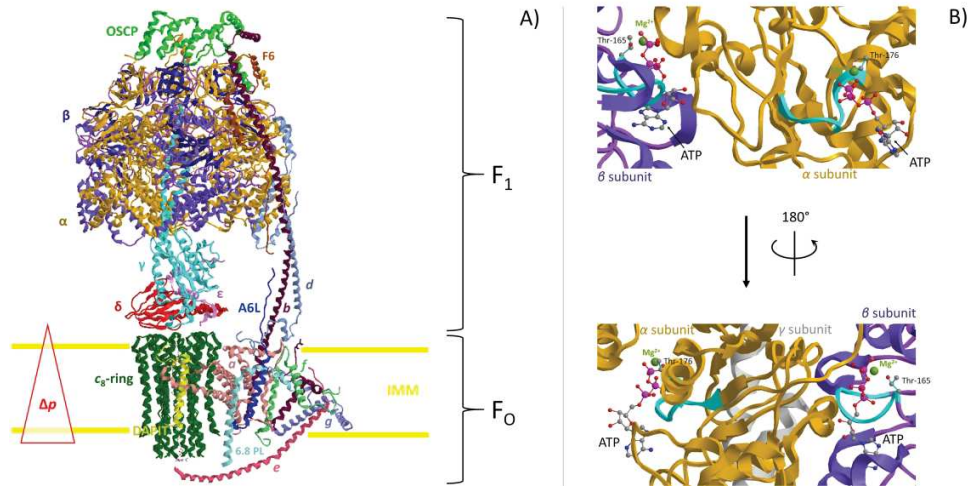


Figure 1. Representative structure of F1FO-ATPase monomers in mammalian mitochondria (A). The enzyme subunits are drawn as ribbon representations obtained from modified PDB ID codes: 6TT7.  $\Delta p$ , Mitchell's proton motive force, IMM, inner mitochondrial membrane. The letter colors are the same as those of the subunit to which belong. B) Catalytic binding site of F1FO-ATPase. The ATP substrate and Mg<sup>2+</sup> cofactor (in ball and stick representation) are located in the  $\beta$  and  $\alpha$  subunits, drawn as ribbon model (modified PDB ID code: 6J5J) in  $\beta$ TP and  $\alpha$ TP conformation, respectively, which show the position of key amino acid residues that bind Mg<sup>2+</sup>. The P-loop is in light blue in both subunits. The binding sites are viewed from the  $\gamma$  subunit (upper panel) and between the observer and the  $\gamma$  subunit (lower panel).

455x229mm (300 x 300 DPI)

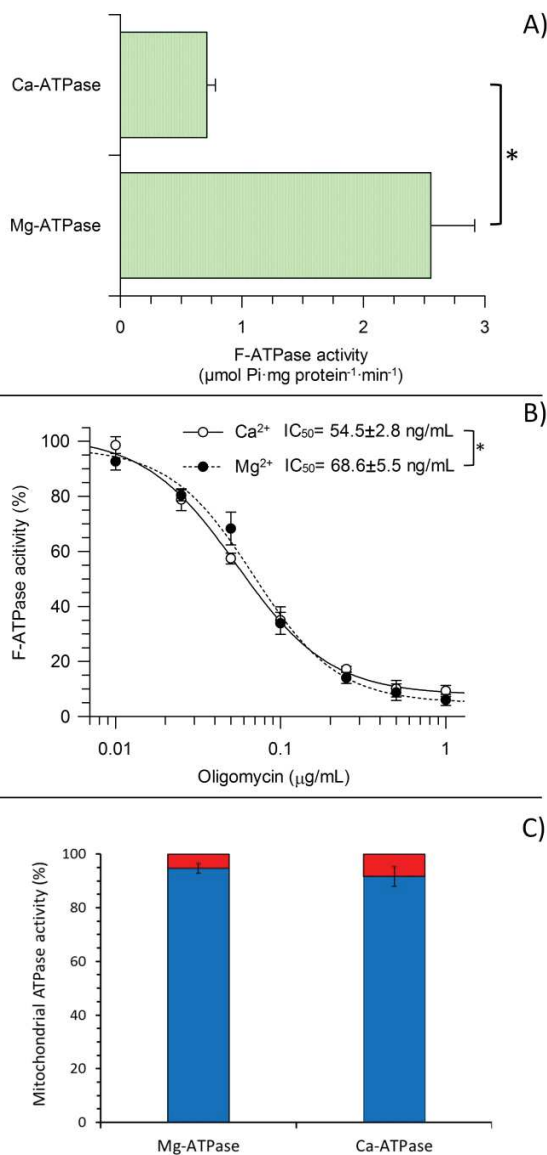


Figure 2. Effect of divalent cations on ATP hydrolysis by the mitochondrial F1FO-ATPase. A) F-ATPase activities in the presence of Ca<sup>2+</sup> or Mg<sup>2+</sup> are shown as bar chart. B) Dose-response curve of oligomycin on the F1FO-ATPase activated by Ca<sup>2+</sup> or Mg<sup>2+</sup> expressed as percentage of the enzyme activity in the absence of oligomycin. C) The oligomycin-sensitive ATPase activity (■ blue) and the oligomycin-insensitive ATPase activity in presence of 3  $\mu\text{g/ml}$  of oligomycin (■ red) are expressed as percentages of the total mitochondrial ATPase activity sustained by Ca<sup>2+</sup> or Mg<sup>2+</sup>, respectively. Data expressed as column chart represent the mean  $\pm$  SD (vertical bars) from three experiments carried out on different mitochondrial preparations. \* indicates significantly different values ( $P \leq 0.05$ ).

100x197mm (600 x 600 DPI)

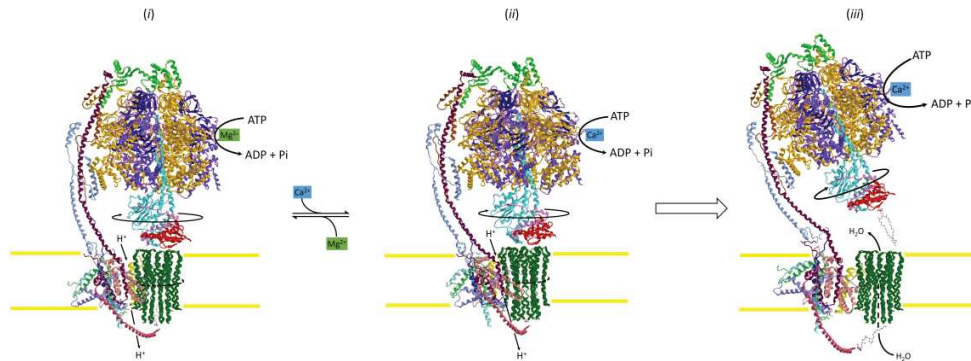


Figure 3. F1FO-ATPase activity raised by Mg<sup>2+</sup> or Ca<sup>2+</sup> as cofactors. ATP hydrolysis sustained by Mg<sup>2+</sup> (i) or Ca<sup>2+</sup> (ii) is coupled to H<sup>+</sup> translocation. The different size of the two cofactors changes the F1FO-ATPase conformation. Indeed, the transition of the Ca<sup>2+</sup>-dependent F1FO-ATP(hydrol)ase from the assembled (ii) to the disassembled state (iii) could induce the loss of H<sup>+</sup>-translocation. Consequently, the PTP opens when a retracted e subunit pulls the lyso-phosphatidylserine plug out of the c-ring at the inner mitochondrial membrane side, while the F1FO destabilization pulls out phosphatidylserine at the matrix side.

381x143mm (600 x 600 DPI)